

## Collective Hamiltonians in the generator coordinate method: A numerical procedure

D. Galetti and S. S. Mizrahi

*Instituto de Física Teórica—Rua Pamplona, 145, Caixa Postal 5956, 01405—São Paulo, Brazil*

(Received 26 August 1981)

A numerical procedure is introduced which allows us to extract a collective Hamiltonian, expressed in terms of a collective canonical pair  $\hat{p}$  and  $\hat{q}$ . The starting point is a microscopic many-body approach, namely the generator coordinate method, and the Weyl formalism permits the description of the collective dynamics in the  $p$ - $q$  space. As an illustration we compare numerical calculations with exact results, obtained analytically, for the quadratic energy kernel with the Gaussian overlap approximation case and the Goldhaber-Teller dipole model applied to the  ${}^4\text{He}$  nucleus.

NUCLEAR STRUCTURE Numerical derivation of collective Hamiltonians. Generator coordinate method, Weyl procedure. Comparison with analytical results.

## I. INTRODUCTION

The generator coordinate method (GCM), introduced by Hill and Wheeler,<sup>1</sup> and later improved by Griffin and Wheeler,<sup>2</sup> has proved to be a powerful tool to treat collective motion in a variety of problems in nuclear physics,<sup>3</sup> although it can be used in a wider realm. Apart from the numerous papers devoted to the study of the properties of the basic GCM equation (Griffin-Wheeler equation),<sup>3</sup> the numerical solution of that equation, in specific problems of nuclear structure, has received special attention, mainly since the work by Flocard and Vautherin.<sup>4</sup> In their work, the collective energy spectra and the associated wave functions are the only collective aspects of the many-body problem that are directly accessible. A new approach to the GCM has been developed through a series of papers,<sup>5-7</sup> the aim of which is to implement a full quantum mechanical treatment to the collective motion. In this method a collective subspace of the many-body Hilbert space is constructed by the diagonalization of the GCM overlap kernel, while the collective dynamics is obtained by the projection of the microscopic many-body Hamiltonian onto this collective subspace. With this new construction one is led to a time-independent Schrödinger-type equation with a nonlocal energy kernel, instead of the Griffin-Wheeler equation. Clearly, in a first stage, this equation governing the collective motion per-

mits the determination of the collective energy spectra and the wave functions which correspond to the results obtained by Flocard and Vautherin. However, this formalism still permits one to identify explicitly an essential dynamical ingredient of the motion, namely, the collective Hamiltonian. This can be achieved by the use of the Weyl transformation,<sup>8</sup> exploring the nonlocal character of the energy kernel. The procedure which allows the construction of a quantum collective Hamiltonian, written in terms of a canonical pair  $\hat{p}$ - $\hat{q}$ , has been developed and some analytical applications were presented in Ref. 9.

In order to treat problems which cannot be solved analytically, a numerical calculational scheme must be worked out. It is the aim of this paper to present such a numerical procedure as an alternative approach to obtain the desired quantities related to the collective motion. Since this procedure is useful in problems that cannot be solved analytically, it is important to establish reliability criteria and limits of applicability of the method and these are illustrated by comparing the results thus obtained with the exact solution in two simple cases, the Gaussian overlap approximation with quadratic energy kernel (GOA), and the dipole giant resonance in the Goldhaber-Teller model for the  ${}^4\text{He}$  nucleus.

In Sec. II we briefly discuss and derive the main equations for the numerical treatment of the GCM; the Weyl formalism through which the collective

Hamiltonian can be constructed is presented in Sec. III in its analytical and approximated numerical form. Section IV is devoted to the calculations and comparison with analytical results for the two cases cited. Finally, the conclusions are presented in Sec. V.

## II. DISCRETE GENERATOR COORDINATE METHOD VERSION

As in any numerical calculation, in the GCM we must use a discrete expression for the one real parameter continuous Griffin-Wheeler (GW) ansatz

$$|\Psi\rangle = \int d\alpha |\alpha\rangle f(\alpha), \quad (1)$$

where  $\alpha$  is the generator coordinate (GC), i.e.,

$$|\Psi\rangle = \sum_i f_i |\alpha_i\rangle \quad (2)$$

so that the GW equation

$$\int [\langle\alpha|\hat{H}|\alpha'\rangle - E\langle\alpha|\alpha'\rangle] f(\alpha') d\alpha' = 0 \quad (3)$$

in the discretized version becomes

$$\sum_{j=1}^N (H_{ij} - EN_{ij}) f_j = 0, \quad i=1,2,\dots,N, \quad (4)$$

where  $H_{ij}$  and  $N_{ij}$  are elements of the matrices defining the energy and overlap kernels, respectively. We must emphasize that in Eq. (4) the GC does not appear explicitly anymore, but it occurs as a multiple of a previously defined constant through the indexes  $i$  and  $j$ . Hereafter we will refer to this constant as the step. Now, through proper transformations we project the discrete GW equation in the collective subspace<sup>6</sup> following the steps below.

(i) Diagonalization of the overlap kernel  $\underline{N}$

$$\underline{U}^\dagger \underline{N} \underline{U} = \underline{\lambda}, \quad (5)$$

where  $\lambda_i$  are the corresponding eigenvalues. As an inherent feature of the method proposed here, the choices of the step and the interval of variation of the GC are intimately related to the spectrum of the resulting eigenvalues  $\{\lambda_i\}$ , i.e., given a small number  $\epsilon$  we must get  $\epsilon < \min\{\lambda_i\}$  by a convenient choice of the above numerical parameters.<sup>4</sup> It is important to stress that as the  $\lambda_i$ 's are the norm of the collective states,<sup>5</sup>  $\epsilon$  is chosen in order to avoid a true null space besides numerical errors.

(ii) The formal expression

$$(\underline{N}^{-1/2} \underline{H} \underline{N}^{-1/2} - E)(\underline{N}^{1/2} f) = 0 \quad (6)$$

can be interpreted in terms of a collective subspace as

$$(\underline{\lambda}^{-1/2} \underline{\tilde{H}} \underline{\lambda}^{-1/2} - E) \underline{g} = 0, \quad (7)$$

where

$$\underline{\tilde{H}} = \underline{U}^\dagger \underline{H} \underline{U}, \quad (8)$$

and

$$\underline{g} = \underline{U}^\dagger (\underline{N}^{1/2} f). \quad (9)$$

Equation (7) is an eigenvalue problem whose diagonalization gives the collective energy spectrum  $\{E_i\}$  and eigenfunctions  $g$ 's.

Until now the scheme presented is the standard one,<sup>4</sup> and does not allow us to extract any information about a collective potential and inertia function. This, however, can be achieved through the Weyl formalism.<sup>8</sup>

## III. WEYL FORMALISM

In a previous paper<sup>9</sup> it was shown that a collective Hamiltonian can be extracted from the continuous version of the nonlocal energy kernel in the collective subspace,

$$\langle k | \hat{H} | k' \rangle \leftrightarrow \underline{\lambda}^{-1/2} \underline{\tilde{H}} \underline{\lambda}^{-1/2},$$

by the use of Weyl's transformation. However, it will be more convenient to work here in a representation labeled by the GC itself. This can be done, in the continuous version, by a double Fourier transformation, whereas in the discrete case we perform the  $\underline{U}$  transformation

$$\langle x | \hat{H} | x' \rangle \leftrightarrow (\underline{U} \underline{\lambda}^{-1/2} \underline{\tilde{H}} \underline{\lambda}^{-1/2} \underline{U}^\dagger)_{ij} \equiv K_{ij}. \quad (10)$$

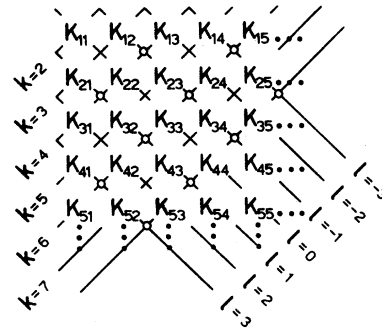


FIG. 1. The relationship between the matrix elements  $K_{ij}$  and the entities  $\mathcal{X}_{kl}$ .

The usual label transformation

$$\frac{x+x'}{2} = q, \quad x-x' = \xi, \quad (11)$$

has a correspondent in the discrete case through the following redefinition of indexes,

$$i+j=k, \quad i-j=l; \quad (12)$$

thus we can rewrite the continuous and discrete kernels (10) into the new form

$$\left\langle q + \frac{\xi}{2} \left| \hat{H} \right| q - \frac{\xi}{2} \right\rangle \leftrightarrow \mathcal{K}_{kl}. \quad (13)$$

The relationship between the matrix elements  $K_{ij}$  and the entities  $\mathcal{K}_{kl}$  can be seen in pictorial form in Fig. 1, where the following correspondence holds

$$\begin{array}{lll} K_{1,1} = \mathcal{K}_{2,0} & K_{2,1} = \mathcal{K}_{3,1} \cdots & K_{N,1} = \mathcal{K}_{N+1,N-1} \\ K_{1,2} = \mathcal{K}_{3,-1} & K_{2,2} = \mathcal{K}_{4,0} \cdots & \vdots \\ \vdots & \vdots & \vdots \\ K_{1,N} = \mathcal{K}_{N+1,1-N} & \cdots & K_{N,N} = \mathcal{K}_{2N,0} \end{array}$$

In the above continuous kernel,  $q$  is identified as the dynamical variable associated with the collective coordinate  $\hat{q}$  of the collective Hamiltonian, while  $\xi$  is a nonlocal parameter which will be in-

tegrated over in the Weyl scheme. In turn, the elements  $\mathcal{K}_{kl}$  do not form a matrix in the usual sense if the matrix (10) is of finite dimension; they only constitute an array of numbers that will be handled according to the procedure to be presented.

Now, the Weyl transformation of the collective Hamiltonian we are looking for is associated with the continuous energy kernel (13) through

$$h_w(q,p) = \int e^{i(p\xi/\hbar)} \left\langle q + \frac{\xi}{2} \left| \hat{H} \right| q - \frac{\xi}{2} \right\rangle d\xi. \quad (14)$$

The right hand side of this expression can be written in the more convenient form

$$h_w(q,p) = \sum_{n=0}^{\infty} \left[ -\frac{i}{\hbar} \right]^n p^n H^{(n)}(q), \quad (15)$$

where we have expanded the exponential in a power series of  $p$ , and

$$H^{(n)}(q) = \frac{(-1)^n}{n!} \int d\xi \xi^n \left\langle q + \frac{\xi}{2} \left| \hat{H} \right| q - \frac{\xi}{2} \right\rangle \quad (16)$$

are the moments of the expansion, in terms of which the collective Hamiltonian will be written:

$$\hat{H}_c(\hat{q}, \hat{p}) = \hat{H}^{(0)}(\hat{q}) + \sum_{n=1}^{\infty} \frac{(-i)^n}{(2\hbar)^n} \left\{ \left\{ \dots, \left\{ \hat{H}^{(n)}(\hat{q}), \hat{p} \right\}, \dots, \hat{p} \right\} \right\} \quad (n \text{ anticommutators}). \quad (17)$$

The  $\hat{H}^{(0)}(\hat{q})$  term corresponds to the velocity-independent collective potential and  $\hat{H}^{(2)}(\hat{q})$  is identified as a collective inertia function. Although the collective Hamiltonian is described by the full series (17), in certain cases the first two moments are sufficient to give a good description of the collective dynamics, and even a natural truncation may occur.

Guided by analogy, the corresponding moments in the discrete case are given by the ansatz

$$H_{k/2}^{(n)} = \sum_l [\mathcal{K}_{kl} \delta_{l,\text{even}} + I_{kl}(\mathcal{K}_{k-1,l}; \mathcal{K}_{k+1,l}) \delta_{l,\text{odd}}] \frac{(l\Delta)^n}{n!}, \quad \frac{k}{2} = 1, 2, \dots, N \quad (18)$$

for even  $k$ , where  $\Delta$  is the step,  $N$  is the order of the matrix  $\underline{K}$  and the  $I_{kl}(\mathcal{K}_{k-1,l}; \mathcal{K}_{k+1,l})$ 's correspond to numbers calculated by interpolation (quadratic in our choice) along the lines of fixed values of odd  $l$ , and for odd indexes  $k-1$  and  $k+1$ . This particular choice for the interpolation along a line of fixed odd  $l$  is convenient since the sequence of points along this same line describes a smooth curve. The location of these new values in Fig. 1 correspond to the crossings of the lines marked by circles, i.e., each  $I_{kl}$  is symmetrically located between  $\mathcal{K}_{k-1,l}$  and  $\mathcal{K}_{k+1,l}$ . The numbers

$I_{kl}$  do not appear naturally in the array for odd values of  $l$ , so they must be introduced in the sum (18); otherwise the moments would miss information if only even  $l$ 's were considered. Therefore the numerical values of  $H_{k/2}^{(n)}$  are expected to be in close agreement with the values of the exact  $H^{(n)}(q)$  (calculated at the same point,  $q = k\Delta/2$ ) when precise numerical calculations are performed.

The discrete procedure clearly constitutes a practical approach to the Weyl scheme; in fact, the appearance of discrepancies between the analytically calculated moments (16) and the numerically calcu-

lated ones (18) are due to two independent motives:

(a) numerical errors, present in any numerical calculation;

(b) the finiteness and discretization of the selected interval of variation of the GC, inherent to the numerical procedure.

An analysis of the performance of the numerical procedure can be accomplished through a comparison of the numerical moments with the exact ones in cases when the latter are available. This analysis has been done with the aid of two examples to be described in the next section. The main feature drawn from this analysis is that the scheme for the numerical calculations must contain three general requirements to be satisfied if we want to obtain a good agreement with an exact solution, namely.

(i)  $\epsilon < \min \{ \lambda_i \}$ ,  $\epsilon$  being a number of the order of the precision required (limited by the computer precision), as already mentioned;

(ii) the highest density of points allowed by the width of the GCM overlap kernel<sup>6,11</sup> must be reached;

(iii) the sum (18) has to present convergence.

These three requirements will constitute a guide at our disposal to attain reliable numerical results even for problems where an exact treatment is not possible.

#### IV. APPLICATIONS

##### A. The harmonic oscillator (HO)

We have chosen the simplest analytical example, the harmonic oscillator, in order to test the numerical procedure and to compare the results with the exact ones. The adopted overlap and energy kernels are

$$N(\alpha, \alpha') = \exp \left[ -\frac{(\alpha - \alpha')^2}{b^2} \right] \quad (19)$$

and

$$H(\alpha, \alpha') = N(\alpha, \alpha') \left[ E_0 + \frac{c_1}{2} (\alpha - \alpha')^2 + \frac{1}{2} c_2 \left[ \frac{\alpha + \alpha'}{2} - \gamma_0 \right]^2 \right], \quad (20)$$

respectively.<sup>2</sup> In the Weyl formalism presented in Ref. 9, these expressions give rise to the collective Hamiltonian

$$\hat{H}_{\text{coll}}(\hat{q}, \hat{p}) = E_0 + \left[ \frac{c_2}{16} - \frac{c_1}{4} \right] b^2 + \frac{c_2}{4} (\hat{q} - \gamma_0)^2 + \frac{\hat{p}^2}{2M_{\text{coll}}}, \quad (21)$$

where

$$M_{\text{coll}} = -\frac{4\hbar^2}{c_1 b^4} \quad (22)$$

is the  $\hat{q}$ -independent collective mass.

In this particular case, only the zeroth and second moments are present in the collective Hamiltonian; the remaining moments vanish identically. The comparison between the numerical results and the exact ones is presented in Figs. 2 and 3. The points depicted correspond to the relative deviation  $\gamma_k^{(n)}$ , defined as

$$\gamma_k^{(n)} = 1 - \frac{H_{\text{exact}}^{(n)} \left[ \frac{k\Delta}{2} \right]}{H_{k/2, \text{numerical}}^{(n)}}. \quad (23)$$

The curves exhibited in Fig. 2, corresponding to the collective potential, were obtained with the following values of the parameters appearing in expressions (21) and (22):  $b^2 = 0.0759 \text{ fm}^2$ ,  $E_0 = -25 \text{ MeV}$ ,  $c_1 = -1250 \text{ MeV fm}^{-2}$ ,  $c_2 = 500 \text{ MeV fm}^{-2}$ , and  $\gamma_0 = 1.0 \text{ fm}$ ; the value for  $\epsilon$  was taken as  $1 \times 10^{-5}$ . The three curves were constructed with a fixed range of variation of the GC (4 fm), while, for the step, three different values were assigned, leading to matrices the order of which are  $N = 20, 25$ , and  $35$  for curves (a), (b), and (c), respectively.

Although the relative deviations are rather small in the three curves (less than 1% in the central part of the collective potential), it is important to note that the greater the order of the matrices involved in each case, the smaller will be the deviations from the exact curves; this is due to a greater number of terms in the sum (18). In every curve more pronounced deviations occur at the border points of the interval, due to the reduced number of terms available for the sum (18); this is a natural consequence of the finite dimension of the matrices involved, thus leading to a poor convergence. With this observation we are able to establish a guiding rule, namely, the border points must be dropped out in this kind of numerical calculations since, surely, the errors contained in them will be greater than those errors of the central points. The departure of smoothness in the central part of the curves (a) and (b) is due to the near zero values of the numerically calculated points, thus enhancing

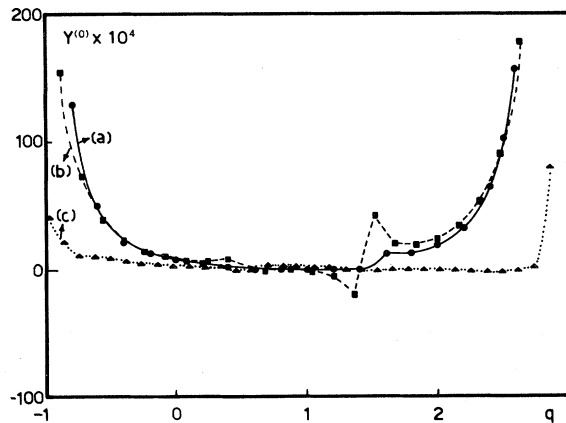


FIG. 2. The curves a, b, and c correspond to the relative deviations of the zeroth moment  $\gamma_k^{(0)}$  for the HO, calculated numerically at the points indicated, for  $N=20$ , 25, and 35, respectively.

the relative deviation  $\gamma_k^{(n)}$ .

In Fig. 3 the relative deviations for the second moment for the cases  $N=20$  and  $N=35$  points are exhibited. It can be seen that, for given  $N$ , the relative deviation is much more pronounced than that calculated for the corresponding zeroth moment for the same number of terms of the sum (18). This is due to the weight factor  $(l\Delta)^2/2$  which tends to enhance the importance of the terms with  $|l|$  near or equal to  $\max |l|$  (for a given  $k$ ), thus leading to a slower convergence of (18). Furthermore, greater errors will be carried into  $H_{k/2}^{(2)}$ , since these terms are of the order of magnitude of the errors involved.

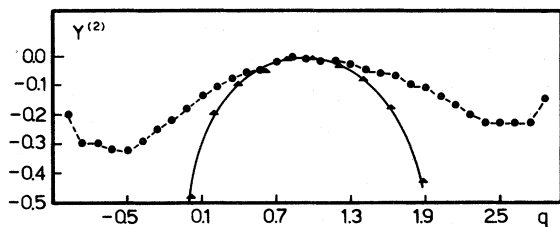


FIG. 3. The curves corresponding to the sequences of triangles and dots correspond to the relative deviations of the second moment  $\gamma_k^{(2)}$  for the HO, for  $N=20$  and 35, respectively.

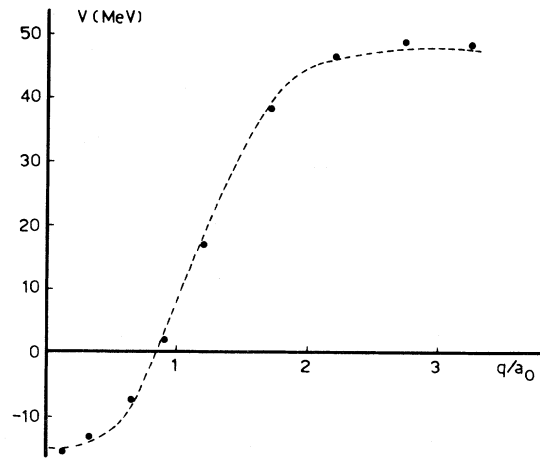


FIG. 4. The dashed curve represents the collective potential for the dipole giant resonance of the  ${}^4\text{He}$  nucleus as analytically calculated in Ref. 10; the dots correspond to the numerical calculations.

#### B. Dipole giant resonance (Goldhaber-Teller model) ${}^4\text{He}$

This problem has been treated analytically in Ref. 10. The GCM overlap and energy kernels are those calculated by Flocard and Vautherin,<sup>4</sup> where the Skyrme interaction SIII was used. The GC adopted here is the separation between the centers of mass of the proton and the neutron densities. The zeroth moment corresponding to the collective potential has the explicit form

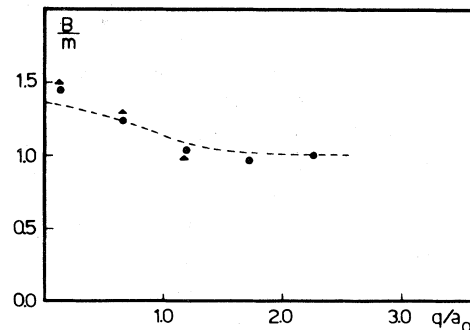


FIG. 5. The dashed curve represents the inertia function, in units of the nucleon mass, for the dipole giant resonance of the  ${}^4\text{He}$  nucleus as analytically calculated in Ref. 10. The triangles and the dots correspond to the numerical calculations performed in simple and double precision, respectively.

$$\begin{aligned}
H^{(0)}(q) = & t_0 \left[ 1 + \frac{x_0}{2} \right] \frac{2}{\pi^{3/2} a_0^3} (e^{-q^2/a_0^2} - 2^{-1/2}) + \frac{t_1 + t_2}{2\pi^{3/2} a_0^5} \left[ \left( 1 + \frac{2q^2}{a_0^2} \right) e^{-q^2/a_0^2} - 3 \times 2^{-3/2} \right] \\
& + \frac{t_2 - 3t_1}{\pi^{3/2} a_0^5} \left[ \left( \frac{q^2}{a_0^2} - 1 \right) e^{-q^2/a_0^2} + 3 \times 2^{-5/2} \right] + \frac{4t_3}{3\pi^3 a_0^6} (e^{-2q^2/a_0^2} - 3^{-1/2}) \\
& - \frac{\hbar^2}{4a_0^2 \mu} \left[ 1 + \frac{m_n(t_1 + t_2)}{\pi^{3/2} \hbar^2 a_0^3} e^{-q^2/a_0^2} \right]. \tag{24}
\end{aligned}$$

The expression for the second moment, which is related to the collective mass, is

$$H^{(2)}(q) = \frac{1}{\mu} \left[ 1 + \frac{m_n(t_1 + t_2)}{\pi^{3/2} \hbar^2 a_0^3} e^{-q^2/a_0^2} \right]. \tag{25}$$

In the above expressions (24) and (25),  $a_0$  is the HO constant,  $m_n$  is the nucleon mass, and  $\mu$  is the reduced mass of the system composed of a cluster of protons and a cluster of neutrons. The remaining parameters are those of the Skyrme force.<sup>4</sup>

The comparison between the exact analytical expression and the numerical results is shown in Figs. 4 and 5 for the zeroth and second moments, respectively. The numerical work was carried out with the following set of parameters:

- (i)  $N=20$ ;
- (ii) interval of variation of the GC, from  $-6.2$  to  $9.0$  fm;
- (iii) step =  $0.8$  fm.

In this realistic case we have done the numerical calculations in simple and also in double precision, in order to compare the results when numerical errors are diminished. In simple precision we obtained nine and three points, presenting convergence, for the zeroth and second moments, respectively. The double precision calculations do not modify significantly the values of the zeroth moment points (obtained in simple precision), giving exactly the same nine points; however, it improves the results for the second moment leading now to five points presenting convergence and also getting closer to the analytical curve.<sup>12</sup>

## V. CONCLUSIONS

We have presented a numerical procedure the aim of which is to calculate the coefficients associated to a collective Hamiltonian expansion. This Hamiltonian is obtained via the GCM and the Weyl formalism and is written in terms of a canonical pair  $\hat{p}\text{-}\hat{q}$  for a single real GC  $\alpha$ .

In practical problems, when an analytical solu-

tion cannot be obtained, this procedure constitutes a valuable alternative approach. Because of the necessity of a numerical calculation, Weyl's actual scheme of quantization is substituted by an approximation due to the introduction of the discretization scheme.

An analysis of the performance of the procedure was done in the GOA with the quadratic energy kernel, whose analytical solution is the well known HO. We showed in this practical example how to attain least deviations between the exact and numerical calculated zeroth and second moments, for different step values and a fixed interval of variation of the GC, and we have depicted the relative deviations. Diminishing the step further, or equivalently increasing the order of the matrices, in the same range of 4 fm, numerical errors will be introduced, since, at least,  $\min \{ \lambda_i \}$  becomes very small (of the order of the numerical precision adopted) and will contain important sources of error. For the higher moments, the relative deviations are more pronounced since they contain greater errors due to the term  $(l\Delta)^n/n!$  present in (18); this effect can be seen in Fig. 3. This trend can be diminished by increasing the computational precision, thus decreasing the errors contained in the elements  $\mathcal{X}_{kl}$ .

As a general feature of the numerical procedure, the step turns out to be of the order of the overlap kernel width<sup>11</sup> when a best agreement between numerical and exact curves is achieved. This fact is reflected in actual problems when the overlap kernel width happens to be large, then a natural limitation for the step emerges, leading to a low density of points in the interval. However, in particular cases of translationally invariant overlap kernels, intermediate points can be generated by convenient shifts of the interval of variation of the GC.

The <sup>4</sup>He dipole giant resonance case constitutes a less trivial application, although it possesses an analytical solution. Here also the numerical calculations presented satisfactory agreement with the analytical results, and particularly it was verified

that a double precision calculation improves the second moment agreement.

We want to emphasize that our primordial objective was *not* the search for higher precision numerical values in the two illustrative examples, but was rather to present a numerical procedure to obtain collective Hamiltonians and discuss its advantages and limitations in order to warrant reliance in problems for which analytical solutions are not available for comparison.

In a forthcoming publication we will present the

results, using this numerical procedure, in a problem whose exact solution we could not reach, namely, the collective potential and inertia function for the two alpha decay of the  $^8\text{Be}$  nucleus.

The authors thank Professor A. F. R. de Toledo Piza and Dr. E. J. V. Passos from Universidade de São Paulo for helpful discussions and critical reading of the manuscript. This work was supported by FINEP under Contract B/76/80/146/00/00 and CNPq, Brazil.

---

<sup>1</sup>D. Hill and J. A. Wheeler, Phys. Rev. **89**, 1102 (1953).

<sup>2</sup>J. J. Griffin and J. A. Wheeler, Phys. Rev. **108**, 311 (1957).

<sup>3</sup>C. W. Wong, Phys. Rep. **15C**, 283 (1975).

<sup>4</sup>H. Flocard and D. Vautherin, Nucl. Phys. **A264**, 197 (1976).

<sup>5</sup>A. F. R. de Toledo Piza *et al.*, Phys. Rev. C **15**, 1477 (1977).

<sup>6</sup>A. F. R. de Toledo Piza and E. J. V. Passos, Nuovo Cimento **45B**, 1 (1978).

<sup>7</sup>E. J. V. Passos and A. F. R. de Toledo Piza, Phys.

Rev. C **21**, 425 (1980).

<sup>8</sup>H. Weyl, Z. Phys. **46**, 1 (1927).

<sup>9</sup>D. Galetti and A. F. R. de Toledo Piza, Phys. Rev. C **24**, 2311 (1981).

<sup>10</sup>E. J. V. Passos and F. F. S. Cruz, Phys. Rev. C **24**, 690 (1981).

<sup>11</sup>D. Galetti and A. F. R. de Toledo Piza, Phys. Rev. C **17**, 774 (1978).

<sup>12</sup>All calculations were carried out on the Universidade de São Paulo's Burroughs 6700 computer.